Polymer 100 (2016) 169–178

Contents lists available at ScienceDirect

Polymer

journal homepage: www.elsevier.com/locate/polymer

Nanocomposite DNA hydrogels with temperature sensitivity

Ahmet T. Uzumcu, Orhan Guney**, Oguz Okay*

Istanbul Technical University, Departments of Chemistry and Polymer Science & Technology, 34469, Maslak, Istanbul, Turkey

ARTICLE INFO

Article history:
Received 27 June 2016
Received in revised form
9 August 2016
Accepted 11 August 2016
Available online 13 August 2016

Keywords:
DNA
Nanocomposite hydrogels
Denaturation
Mechanical properties
Swelling

ABSTRACT

DNA hydrogels are promising soft materials because of the distinctive properties of DNA such as biocompatibility, coil-globule transition, molecular recognition, and selective binding. However, such hydrogels synthesized so far suffer from poor mechanical properties and low dimensional stability, which limit their stress-bearing technological applications. Here, we introduce a novel concept for the preparation of high-strength double-stranded (ds) DNA hydrogels with temperature sensitivity. The hydrogels were synthesized by free-radical polymerization of *N*-isopropylacrylamide in aqueous Laponite dispersions containing ds-DNA in a highly entangled state. The nanoparticles of synthetic Laponite clay act as a dynamic cross-linker to form a three-dimensional physical network due to strong clay-polymer interactions. We observed that ds-DNA maintains its native structure and function during the formation of nanocomposite hydrogels. Cyclic heating/cooling experiments conducted between below and above the melting temperature of ds-DNA reveal a drastic increase in the elastic modulus of nanocomposite hydrogels due to the thermally induced denaturation and renaturation of DNA within the physical network. The hydrogels prepared at various Laponite contents display the characteristics of both poly(*N*-isopropylacrylamide) and ds-DNA e.g., temperature sensitivity, denaturation and renaturation of DNA strands, and they exhibit a high tensile fracture stress (up to 53 kPa) and elongation to break (up to 544%).

1. Introduction

Deoxyribonucleic acid (DNA) molecules found in all living cells are carriers of genetic information in their base sequences. DNA is a high-molecular weight biopolymer made from repeating units called nucleotides consisting of deoxyribose sugar, a phosphate group and side group amine bases. When aqueous solutions of double-stranded DNA are heated, the hydrogen bonds keeping the two strands together break and DNA dissociates into single strands with a random coil conformation [1]. This transition from double-stranded (ds) to single-stranded (ss) DNA called denaturation or melting can be reversed by slow cooling of dilute DNA solutions, which is called renaturation [2].

DNA hydrogels are water-swollen three-dimensional networks of DNA strands [3,4]. Such hydrogels are promising soft materials because of the unique properties of DNA such as biocompatibility, discrete conformational transition between a random coil and a compact globule induced by the addition of condensation agents, highly selective binding, and molecular recognition [5,6]. DNA hydrogels have a wide range of potential applications including biosensors, gene therapy, drug delivery, and tissue engineering [7–10]. Another advantage of using DNA to make functional and responsive hydrogels is that a large amount of DNA could be recovered at a low price from natural sources such as the industrial wastes of marine products [11]. Due to the double-stranded structure of DNA, chemical compounds having aromatic planar groups such as ethidium bromide (EtBr), a four-ringed aromatic molecule with three of the rings conjugated, intercalate between adjacent base pairs of ds-DNA and result in mutation and endocrine disruption [12–17]. This characteristics of DNA suggests that the hydrogels containing ds-DNA can also be used as selective sorbents for toxic materials [17].

In recent years, a number of strategies have been employed to prepare physically and chemically cross-linked DNA hydrogels [18–29]. It was shown that the semi-dilute solutions of ds-DNA subjected to heating/cooling cycles between below and above its melting temperature produce physical DNA hydrogels due to the formation of hydrogen bonds between strands belonging to different ds-DNA molecules [24–26]. Although physical DNA

* Corresponding author.
** Corresponding author.
E-mail addresses: oguney@itu.edu.tr (O. Guney), okayo@itu.edu.tr (O. Okay).

http://dx.doi.org/10.1016/j.polymer.2016.08.041
0032-3861/

hydrogels are stable in aqueous NaCl solutions, they easily dissolve in water due to the large osmotic pressure of DNA counterions dominating over the elastic response of the physically cross-linked network segments [30]. Chemical DNA hydrogels have been prepared by cross-linking of DNA in aqueous solutions using a chemical cross-linker such as ethylene glycol diglycidyl ether (EGDE) or butanediol diglycidyl ether (BDDE) [18–20,22–24]. The cross-linker molecules containing epoxide groups on both ends react with the amino groups on the nucleotide bases to form a three-dimensional DNA network. The gelation reactions of DNA with diepoxide cross-linkers have also been conducted in frozen aqueous solutions at −18 °C to produce macroporous DNA cryogels suitable as sorbent for the removal of carcinogenic agents from aqueous solutions [17]. Similar to single DNA molecules, DNA hydrogels undergo volume phase transitions in response to external stimuli, such as the solvent composition, the concentrations of inorganic salts, polyamines, cationic macromolecules, or surfactants [18,20,22,23].

However, DNA hydrogels synthesized so far suffer from poor mechanical properties and low dimensional stability which limit their stress-bearing technological applications. This poor mechanical performance is due to the lack of an efficient energy dissipation mechanism in the chemically cross-linked DNA network leading to rapid crack propagation [31,32]. In the past decades, several techniques have been developed to produce mechanically strong synthetic hydrogels [33]. The common strategy underlying these techniques is to create an energy dissipation mechanism in the hydrogels by introducing sacrificial bonds in the chemically cross-linked network [34,35], or by replacing chemical cross-links with the physical ones [36,37]. Haraguchi et al. prepared nanocomposite (NC) hydrogels exhibiting high fracture energies (up to 6.8 kJ m^{-2}) and elongation to break (>1500%) by solution polymerization of hydrophilic monomers in the presence of Laponite nanoparticles as a physical cross-linker, substituting the traditional chemical cross-linkers [38,39]. For example, poly(*N*-isopropylacrylamide) (PNIPA) hydrogels prepared using Laponite cross-linker are up to 1000 times tougher and 50 times stretchable in comparison with conventional PNIPA hydrogels [40–42]. Laponite, a synthetic hectorite clay, forms disc-like particles in water of 1 nm thickness and about 25 nm diameter, with a strongly negative face charge and a weakly, localized positive edge charge. Laponite nanoparticles act as an effective multifunctional dynamic cross-linker in the formation of NC hydrogels due to strong clay-polymer interactions and nanoscale distribution of Laponite within the semi-dilute polymer solution [38–43]. Such nanocomposite hydrogels are attractive for a wide range of applications.

Interactions between DNA molecules and Laponite nanoparticles have rarely been studied. Arfin et al. recently observed strong DNA-Laponite attractive interactions in aqueous solutions containing 1 w/v% Laponite and 1–1.6 w/v% DNA, suggesting electrostatic binding of DNA to the positively charged edges of Laponite [44]. Taki et al. also reported the existence of strong interactions between DNA molecules and Laponite surfaces leading to the formation of viscoelastic gels [45]. Inspired by these previous works, we introduce here a novel concept for the preparation of high-strength DNA hydrogels with temperature sensitivity. The supramolecular hydrogels consist of in situ formed PNIPA chains, and ds-DNA strands together with Laponite nanoparticles acting as a dynamic multifunctional cross-linker. They were synthesized by free-radical polymerization of *N*-isopropylacrylamide (NIPA) in aqueous Laponite dispersions containing ds-DNA in a highly entangled state. As will be seen below, the native double-stranded DNA conformation remains intact during the formation of nanocomposite hydrogels. The hydrogels prepared at various Laponite contents display the characteristics of both PNIPA and ds-DNA e.g., temperature sensitivity, denaturation and renaturation of ds-DNA strands. They also exhibit a high tensile fracture stress (up to 53 kPa) and elongation to break (up to 544%) as compared to the covalently cross-linked DNA hydrogels.

2. Experimental section

2.1. Materials

Deoxyribonucleic acid sodium salt (DNA) of salmon testes was purchased from Sigma-Aldrich Co. It is a linear, double-stranded DNA of molecular weight 1.3×10^6 g mol^{-1}, corresponding to about 2000 base pairs. The melting temperature of the DNA is 87.5 °C in 0.15 M sodium chloride plus 0.015 M sodium citrate. The synthetic hectorite clay, Laponite XLG ($Mg_{5.34}Li_{0.66}Si_8O_{20}(OH)_4Na_{0.66}$) was provided by Rockwood Ltd. The monomer *N*-isopropylacrylamide (NIPA, Sigma-Aldrich) was recrystallized from toluene/cyclohexane (40/60 v/v) and then dried under vacuum. Potassium persulfate (KPS, Fluka), N,N,N′,N'-tetramethylethylenediamine (TEMED, Sigma-Aldrich), butanediol diglycidyl ether (BDDE, Sigma-Aldrich), and ethidium bromide (Sigma-Aldrich) were used as received.

2.2. Hydrogel preparation

Nanocomposite DNA hydrogels were synthesized at 20 °C by polymerization of NIPA using KPS–TEMED redox initiator system in aqueous Laponite dispersions containing ds-DNA. The initial concentration of the monomer NIPA and the DNA concentration were set to 1 M and 2 w/v%, respectively, while the Laponite concentration was varied between 0.8 and 6.9 w/v%. Laponite XLG was first dissolved in deionized water under vigorous stirring for 1 h. After addition and dissolving NIPA for 15 min, DNA was added into this solution and stirred for 18 h at room temperature to obtain a homogeneous solution. Note that a homogeneous solution could not be obtained at Laponite contents above 6.9 w/v% due to the high solution viscosity. The initiator KPS (3.7 mM) was then added to the viscous solution and stirred in an ice-water bath for 1 h, and finally the accelerator TEMED (0.08 v/v%) was added to initiate the polymerization. The reactions were conducted at 20 °C between the parallel plates of the rheometer as well as in plastic syringes of 4.5 mm internal diameters. In this way, transparent hydrogels were prepared indicating compatibility of DNA with PNIPA and Laponite particles (Fig. S1).

To highlight the effect of DNA on the properties of nanocomposite hydrogels, the polymerization reactions were also conducted in the absence of DNA. To compare the mechanical properties of the present nanocomposite hydrogels with those of the chemically cross-linked DNA hydrogels reported before [24,25], DNA hydrogels were also prepared using BDDE as a chemical cross-linker. Gelation reactions were carried out in aqueous solutions of DNA at a concentration of 6 w/v% in the presence of BDDE cross-linker (17.3 wt% of DNA) and TEMED catalyst (0.44 v/v% of the reaction solution) at 50 °C [24].

2.3. Rheological experiments

Rheological measurements were performed both during and after the polymerization reactions on a Bohlin Gemini 150 rheometer system (Malvern Instruments, UK) equipped with a Peltier device for temperature control. For this purpose, the reactions were carried out at 20 °C between the parallel plates of the rheometer. The upper plate (diameter 40 mm) was set at a distance of 500 μm before the onset of the reactions. During all measurements, a solvent trap was used and the outside of the upper plate

was covered with a thin layer of low-viscosity silicone oil to prevent evaporation of water. An angular frequency of $\omega = 6.3$ rad s^{-1} and a deformation amplitude of $\gamma_o = 0.01$ were selected to ensure that the oscillatory deformation is within the linear regime. Thereafter, frequency-sweep tests at $\gamma_o = 0.01$ were carried out at 20 °C. The heating/cooling cycles were conducted by heating the gel samples from 20 to 90 °C with a rate of 3.25 °C min^{-1}, keeping at 90 °C for 10 min, subsequently cooling down to 20 °C with a rate of 1.08 °C·min^{-1}, and finally keeping at 20 °C for 40 min. The changes in the dynamic moduli of hydrogels were monitored during the course of the heating and cooling scans at $\omega = 6.3$ rad s^{-1} and $\gamma_0 = 0.01$.

2.4. Mechanical tests

Uniaxial compression and elongation tests were performed at 23 ± 1 °C on a Zwick Roell Z0.5 TH test machine using a 500 N load cell. Load and displacement data were collected using cylindrical hydrogel samples of 4.5 mm in diameter and 5 ± 1 mm in length. The stress was presented by its nominal σ_{nom} and true values σ_{true}, which are the forces per cross-sectional area of the undeformed and deformed gel specimen respectively. The true stress σ_{true} was calculated from its nominal value as $\sigma_{true} = \lambda\sigma_{nom}$ where λ is the deformation ratio (deformed length/initial length). The strain was presented by ε, the change in the sample length relative to its initial length, i.e., $\varepsilon = 1\text{-}\lambda$ and $\varepsilon = \lambda\text{-}1$ for compression and elongation, respectively. The Young's modulus E was calculated from the slope of stress–strain curves between 5 and 15% deformations. For uniaxial compression measurements, the hydrogel samples were compressed at a cross-head speed of 15 mm min^{-1}. Before the test, an initial compressive contact to 0.01 ± 0.002 N was applied to ensure a complete contact between the gel and the plates. For uniaxial elongation measurements, the initial sample length between jaws and the cross-head speed were 35 ± 2 mm and 100 mm min^{-1}, respectively.

2.5. Swelling measurements

Cylindrical hydrogel specimens of 4.5 mm in diameter and about 4 cm in length were immersed in a large excess of water at 23 °C for at least 15 days whereby the water was replaced several times to extract any soluble species. The mass m and the diameter D of the gel specimens were monitored as a function of the swelling time. The weight and volume variations were measured by weighing the gel samples and by measuring their diameters using a calibrated digital compass, respectively. The relative weight m_{rel} and volume swelling ratios V_{rel} of the hydrogels with respect to their as-prepared states were calculated as

$$m_{rel} = m/m_0 \tag{1a}$$

$$V_{rel} = (D/D0)^3 \tag{1b}$$

where m_0 and D_o are the initial mass and diameter of the gel sample. Eq (1b) assumes that the hydrogels swell isotropically in all directions, which is generally observed if no internal stress is applied to the gels during their preparation. Then, the samples in equilibrium with pure water were taken out of water and dried at 60 °C under vacuum to constant mass. The gel fraction W_g, that is, the conversion of the reactants (NIPA, Laponite, DNA) to the water-insoluble polymer was calculated from the masses of dry polymer network and of the reactants in the feed solution.

The temperature dependent variation of the swelling ratio of NC hydrogels was measured by immersing the gel samples in a temperature-controlled water bath of 20 ± 0.1 °C. The mass of the gel samples was monitored by weighing the samples until attaining the equilibrium degree of swelling, after which the temperature of the water bath was increased in steps of 2 °C up to 50 °C. The equilibrium weight swelling ratio of the hydrogels at various temperatures was given by m_{norm}, which is the equilibrium swollen mass of the gel sample normalized with respect to its mass at 20 °C.

2.6. Fluorescence measurements

The measurements were carried out using a Varian Cary-Eclipse Luminesce Spectrometer on the reaction mixtures and hydrogels at various reaction times and at various temperatures between 23 and 90 °C. The solutions and gels were immersed in a temperature controlled water tank to adjust the temperature prior to the measurements. Ethidium bromide (EtBr) was used as a fluorescent probe at a concentration of 5 μM. For the measurements, the reaction mixtures were transferred into round glass tubes of 6 mm internal diameter and the polymerization of NIPA was performed in the fluorescence cell of the spectrometer. To distinguish the effects of the reaction components on the conformational changes in DNA, the polymerization reactions were conducted i) in water, ii) in aqueous Laponite dispersions, ii) in 2 w/v% ds-DNA solution, and iv) in aqueous Laponite dispersions containing 2 w/v% ds-DNA. The measurements were performed at an excitation wavelength of 475 nm and then, the emission spectra between 485 and 800 nm were recorded. In order to check whether DNA strands remain completely in the hydrogel during the swelling process or, they are extracted from the gel network, the measurements were also performed on water surrounding the gel samples during the swelling process. For this purpose, about 0.2 g of the gel sample were first immersed into 100 mL water for 7 days without refreshing water. Then, EtBr was added to water samples to make a final concentration of 5 μM EtBr. Assuming that all DNA molecules will diffuse out of the gel phase during swelling, DNA concentration in the external solution will be 40 mg L^{-1}. DNA concentration in the solution was calculated using a calibration curve prepared by titrating of 5 μM EtBr solution by adding ds-DNA.

3. Results and discussion

3.1. Gelation kinetics and rheology of nanocomposite DNA hydrogels

Nanocomposite (NC) hydrogels were synthesized by free-radical polymerization of NIPA in aqueous Laponite dispersions containing 2 w/v% ds-DNA. This concentration of ds-DNA with an average molecular weight of about 2000 base pairs is 47-fold larger than its critical overlap concentration c* (0.043 w/v%) [24]. Thus, ds-DNA in the reaction system is in a highly entangled state, and the polymerization of NIPA occurs in an elastic mesh of DNA. The initial concentration of NIPA was fixed at 1 M while the amount of Laponite was varied between 0.8 and 6.9 w/v%. Because the hydrogels formed at below 2 w/v% Laponite were too weak, we will only discuss the results obtained between 2.3 and 6.9 w/v% Laponite contents.

The formation of nanocomposite hydrogels was monitored by rheometry using oscillatory deformation tests. Fig. 1a shows typical gelation profiles at two different Laponite concentrations, where the elastic modulus G' (filled circles) and the viscous modulus G'' (open triangles) of the reaction system are plotted against the reaction time. Both G' and G'' increase with the reaction time and then they approach plateau values after about 3–4 h. However, with a further increase in the reaction time as indicated by the arrows in Fig. 1a, the dynamic moduli start to

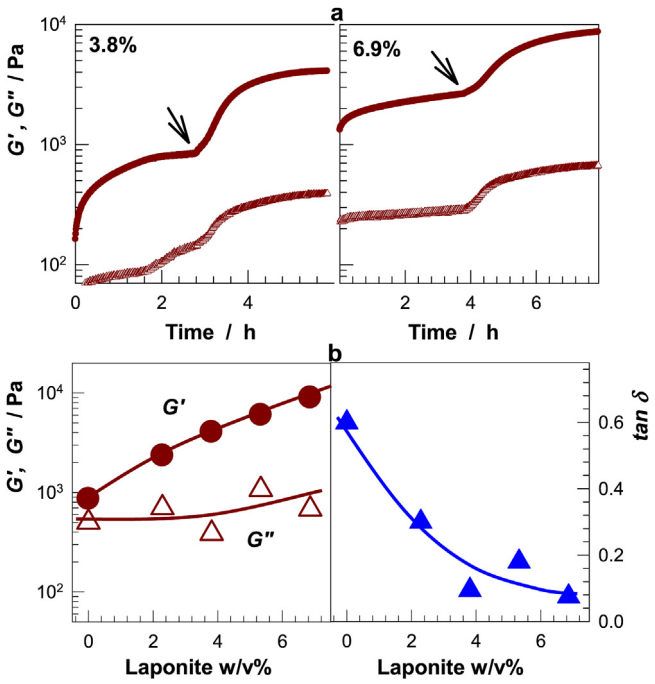

Fig. 1. (a) Elastic modulus G' (filled circles) and viscous modulus G'' (open triangles) of the reaction system shown as a function of the reaction time. NIPA = 1 M. DNA = 2 w/v %. Laponite contents are indicated. $\omega = 6.3$ rad s^{-1} $\gamma_o = 0.01$. (b) G' (filled symbols), G'' (open symbols) and tan δ of the reaction system shown as a function of the Laponite content. The error bars are smaller than the symbols. The curves show the trend of data.

increase again until they approach final plateau values after 6 h. To check whether this autoacceleration in the modulus increase arises due to the presence of DNA, we conducted the gelation reactions in the absence of DNA and observed a similar phenomenon, yet the onset of acceleration was shifted to shorter reaction times (Fig. S2). We attribute the autoacceleration in the modulus increase to the Trommsdorff or gel effect that arises due to the increasing viscosity of the reaction system reducing the probability of termination of the growing chain radicals and thereby increasing the polymerization rate. Such an effect has been observed before during the polymerization of methyl methacrylate in clay dispersions [46]. Moreover, the cross-linking effect of KPS initiator radicals may also be responsible for the modulus increase at long reaction times [47,48]. The shift of the onset of autoacceleration to a shorter reaction time in the absence of DNA is attributed to the higher elastic modulus, i.e., cross-link density of the reaction system without DNA (Fig. S3). In Fig. 1b, G', G'', and the loss factor tan δ ($= G''/G'$) of NC hydrogels after a reaction time of 6 h are plotted against the amount of Laponite. The higher the Laponite content, the higher the elastic modulus G' and the lower the loss factor tan δ indicating that rising Laponite content increases the elastic properties of the hydrogels. As compared to the NC hydrogels prepared in the absence of DNA, the addition of DNA slightly decreased the elastic modulus at high Laponite contents while tan δ remained almost unchanged (Fig. S3).

To find out whether the conformation of double-stranded (ds) native DNA remains intact during the formation of nanocomposite hydrogels, or double strands dissociate into single-stranded (ss) flexible DNA strands, fluorescence measurements were performed using ethidium bromide (EtBr) as a fluorescence probe. EtBr is known to bind to ds-DNA by intercalation between the base pairs and results in a high quantum yield of fluorescence [17,25]. In Fig. 2a, the thin and thick black curves represent the fluorescence spectra of aqueous solutions of 5 μM EtBr at 23 °C in the absence and in the presence of ds-DNA, respectively. DNA concentration is 2 w/v%, as the DNA concentration in the hydrogels. It is seen that, in the presence of DNA, EtBr fluorescence significantly increases and this increase depends on the DNA conformation. The colored curves in Fig. 2a represent the spectra of EtBr in 2 w/v% DNA solution at various temperatures. Upon heating the solution from 23 to 90 °C, ds-DNA dissociates into single strands having a random coil conformation [25], thereby the fluorescence intensity decreases. Thus, any dissociation of ds-DNA into single DNA strands during NC hydrogel formation would lead to a decrease in EtBr intensity.

However, we observed that not only DNA but also Laponite nanoparticles in the reaction system interact with EtBr, similar to the interactions between clay particles and cationic dyes such as crystal violet or brilliant green [49–51], and hence hinder the monitoring of a possible conformational change in DNA during the formation of nanocomposite hydrogels. For instance, the presence of only Laponite resulted in an enhancement of EtBr fluorescence intensity indicating formation of a complex between EtBr and Laponite in the pre-gel solutions. This enhancement is due to the more rigid and hydrophobic environment provided to EtBr by Laponite surfaces and the expelling of water molecules surrounding EtBr, which cause the quenching of EtBr fluorescence [52]. On the other hand, the emission intensity of EtBr further increases with increasing reaction time during the polymerization of NIPA in Laponite dispersions, along with a spectral blue shift from 590 to 575 nm (Fig. S4a). This shift in the fluorescence spectra also indicates that EtBr is in a more hydrophobic environment in the presence of Laponite [53]. When comparing the fluorescence behavior of EtBr in Laponite dispersions with and without DNA, EtBr emission intensity is higher in the absence of DNA (Fig. S4a and b), indicating a stronger surrounding of EtBr by Laponite as compared to DNA.

To elucidate the conformational change in DNA during the polymerization, we therefore conducted the fluorescence measurements on the polymerization system without adding Laponite. Fig. 2b shows the fluorescence spectra of 5 μM EtBr during the polymerization of 1 M NIPA without and with 2 w/v% DNA. The data were recorded at various reaction times between 20 min and 24 h. Fluorescence intensity of EtBr does not change in the absence of DNA while in the presence of DNA, the characteristic peak of DNA-bound EtBr at 597 ± 1 nm appears and its intensity slightly increases with increasing reaction time (inset of Fig. 2b), which we attribute to the increasing viscosity of the PNIPA-DNA system with increasing monomer conversion. The fact that the EtBr intensity does not decrease during the polymerization of NIPA reveals that the double-stranded conformation of DNA is not affected by KPS-TEMED redox initiator system, as well as by the monomer NIPA, and the polymer PNIPA. After a polymerization time of 24 h, fluorescence measurements were performed at various temperatures on the semi-dilute PNIPA-DNA solution, which is the same system as the NC hydrogels except that no Laponite was included. Fig. 2c represents the spectra of PNIPA-DNA solution containing 5 μm EtBr at temperatures between 23 and 90 °C. An abrupt initial decrease in the fluorescence intensity is observable due to the volume-phase transition of PNIPA at around 34 °C [54,55]. However, zooming in to the collapsed region between 50 and 90 °C reveals a decrease in EtBr intensity at 597 nm (inset of Fig. 2c), indicating that DNA in the semi-dilute PNIPA solution dissociates by heating above its melting temperature (87.5 °C). This supports that DNA after the polymerization reaction at 23 °C is in a double-stranded conformation. We conclude that DNA maintains its native structure and function during the formation of NC hydrogels.

After a reaction time of 6 h, dynamic frequency-sweep tests

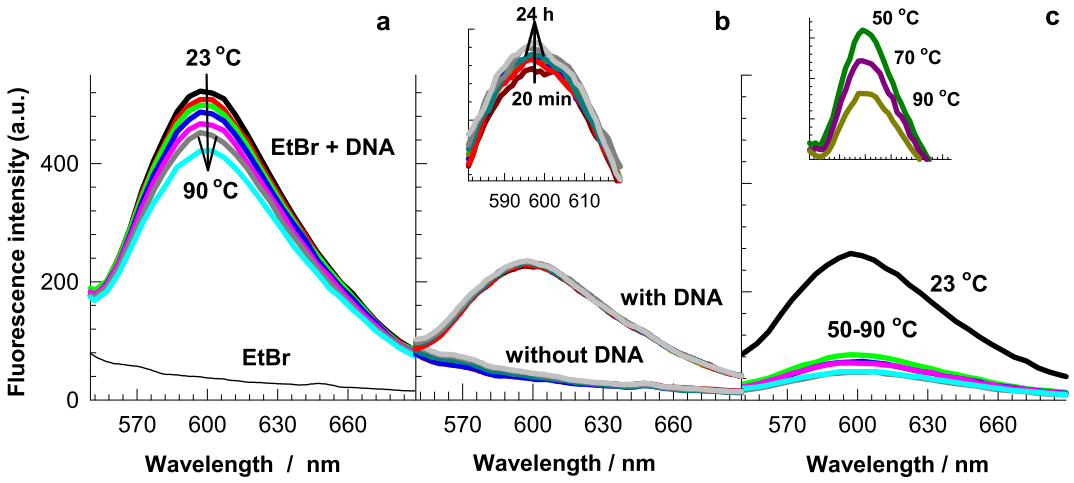

Fig. 2. Fluorescence spectra 5 μM EtBr in different environments. (a) In water without (thin curve) and with 2 w/v% DNA (thick curves) at 23 (black), 40 (red), 50 (green), 60 (blue), 70 (pink), 80 (dark gray), and 90 °C (cyan). (b) During the polymerization of NIPA without and with 2 w/v% DNA. The inset is a zoom-in to the peak region. NIPA = 1 M. KPS = 3.7 mM. TEMED = 0.08 v/v%. Reaction time = 0.33 (dark red), 0.5 (blue), 1 (dark yellow), 2 (red), 3 (pink), 4 (dark cyan), 8 (dark gray) and 24 h (gray). (c) After a polymerization time of 24 h in the presence of 2 w/v% DNA at various temperatures. The inset is a zoom-in to the spectra recorded between 50 and 90 °C. (For interpretation of the references to colour in this figure legend, the reader is referred to the web version of this article.)

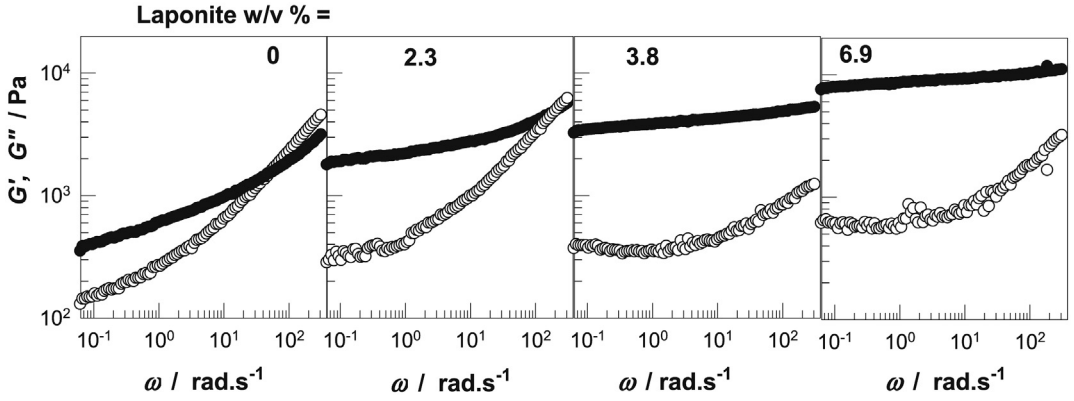

Fig. 3. G' (filled symbols) and G'' (open symbols) of NC hydrogels shown as a function of the frequency ω measured after 6 h of reaction time. $\gamma_o = 0.01$. Laponite contents are indicated.

were carried out to explore the internal dynamics of NC hydrogels. Fig. 3 shows the frequency dependencies of G' (filled symbols) and G'' (open symbols) at a strain amplitude $\gamma_o = 0.01$ for the hydrogels formed at various Laponite contents. In the absence of Laponite, that is, the semi-dilute solution of linear PNIPA and DNA molecules exhibits an elastic character ($G' > G''$) at low frequencies and a predominantly viscous character above the crossover frequency of 52 rad s^{-1} at which G' and G'' intersect. This behavior is opposite to that observed in semi-dilute solutions of most polymers where the viscous and elastic characters appear at below and above the crossover frequency in the viscoelastic spectra, respectively. Such an unusual behavior was reported before in aqueous solutions of sodium alginate – PNIPA [56], hyaluronic acid-graft-PNIPA [57], and methyl cellulose [58]. We attribute this feature to the intermolecular hydrogen bonds between DNA and/or PNIPA molecules acting as physical cross-links and thus, contributing to the elasticity of the hydrogel at a low frequency. Increasing frequency gradually breaks the hydrogen bonds so that the weak gel transforms to a viscous solution. Fig. 3 also shows that the addition of Laponite shifts the crossover frequency outside of the experimental window indicating that the effect of multifunctional Laponite cross-links dominate over the physical cross-links. However, the viscous modulus G'' still rises with frequency implying increasing extent of energy dissipation due to the rearrangement of PNIPA and DNA molecules leading to their sliding past each other at short experimental time scales. Comparison of these results with those obtained without DNA reveal that the elastic modulus becomes less frequency dependent after addition of DNA indicating increasing elastic response of the hydrogels (Fig. S5). We have to mention that the present NC hydrogels consisting of highly negatively charged DNA strands and non-ionic PNIPA chains resemble the classical double-network (DN) hydrogels composed of polyelectrolyte first-network and nonionic second-network components [34,35]. Therefore, we cannot exclude the contribution of double-networking to the energy dissipation mechanism.

3.2. Temperature sensitivity of nanocomposite hydrogels and conformational changes of DNA

PNIPA hydrogels are known to exhibit volume-phase transition in response to temperature changes [54,55]. The temperature sensitivity of NC hydrogels containing DNA was studied using hydrogel samples prepared between the parallel plates of the rheometer. The samples were heated from 20 to 50 °C at a rate of

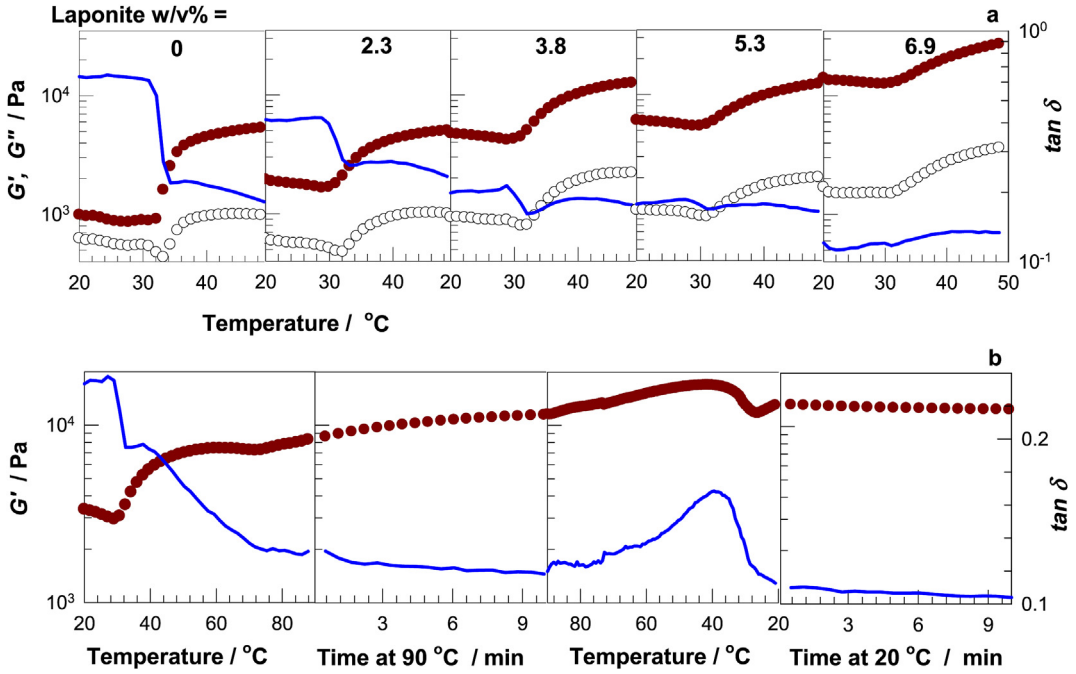

Fig. 4. (a): G' (filled circles), G'' (open circles), and tan δ (lines) of the hydrogels during heating from 20 to 50 °C. Laponite contents are indicated. (b): G' (symbols) and tan δ (lines) of the hydrogel prepared in 3.8 w/v% Laponite during the heating – cooling cycle between 20 and 90 °C. $\omega = 6.3$ rad s^{-1} $\gamma_o = 0.01$.

3.25 °C min^{-1} during which the changes in the dynamic moduli were monitored as a function of temperature. Fig. 4a shows G', G'', and tan δ of the hydrogels with various Laponite contents plotted as a function of the temperature. The elastic modulus G' rapidly increases while the loss factor tan δ decreases at around 32 °C corresponding to the volume-phase transition temperature of PNIPA. The extent of the modulus variation at the transition temperature decreases with rising Laponite content due to the simultaneous increase of the elastic modulus and hence the cross-link density of the hydrogels. The hydrogels were also subjected to cyclic heating/cooling experiments by heating the gel samples above the melting temperature of DNA and subsequently cooling down to 20 °C. Results of the heating/cooling scans between 20 and 90 °C for the NC hydrogel formed at 3.8 w/v% Laponite are shown in Fig. 4b where G' and tan δ are plotted against the temperature. It is seen that the elastic modulus G' of the hydrogel irreversibly increases from 3.3 to 13 kPa while tan δ decreases from 0.24 to 0.10 after the heating/cooling cycle. In contrast, the same hydrogel sample prepared without DNA exhibited a reversible variation in the modulus and loss factor, i.e., the initial modulus G' of 3.5 ± 0.5 kPa and the loss factor tan δ of 0.23 ± 0.03 measured at 20 °C could be recovered after the cycle (Fig. S6). Thus, the presence of ds-DNA in the hydrogel is responsible for the 4-fold increase of the elastic modulus and 2-fold decrease of the loss factor after the heating/cooling cycle between below and above the melting temperature of DNA.

We can explain the drastic increase of the elastic modulus and the decrease of the loss factor after the heating/cooling cycle with the thermally induced denaturation and renaturation of ds-DNA within the physical network, as schematically illustrated in Fig. 5. During the heating period (a→b), the semi-flexible, double-stranded DNA partially dissociates into flexible single-strand fragments so that the number of entanglements between PNIPA and DNA chains increases. On cooling back (b→c), the dissociated DNA strands cannot re-organize to form the initial double-stranded conformation due to the high DNA concentration and thereby the hydrogen bonds formed between different DNA strands act as physical junction zones in addition to the Laponite cross-links. Previous works indeed show formation of physical DNA hydrogel by subjecting semi-dilute DNA solutions to heating/cooling cycles [24–26]. For example, the elastic moduli of aqueous solutions of 1 and 5 w/v% ds-DNA increase from 10 Pa to 100 Pa and from 100 Pa to 19 kPa, respectively, after the heating/cooling cycle between 20 and 90 °C [26].

3.3. Mechanical properties of the hydrogels

After a reaction time of 24 h, NC hydrogels were subjected to uniaxial compression and elongation tests. Fig. 6a represents typical tensile stress-strain data of the hydrogels at 23 ± 1 °C as the dependence of the nominal stress σ_{nom} on the strain ε. It is seen that the initial slope of the stress-strain curves corresponding to the Young's modulus of the hydrogels as well as the stress and strain at fracture increase as the content of Laponite increases. The results of the tensile tests are compiled in Fig. 6b, where the Young's modulus E, fracture stress σ_f, and fracture strain ε_f are plotted against the Laponite content. NC hydrogels with a Young's modulus of 7–30 kPa sustain up to 544% elongations and 53 kPa tensile stresses. For comparison, pure DNA hydrogels were prepared at a DNA concentration of 6 w/v% using BDDE as a chemical cross-linker [24]. These hydrogel samples were too brittle to be held between the two clamps of the test machine. The compression test results are shown in Fig. 6c and d, where the nominal σ_{nom} and true stresses σ_{true} are plotted against the compressive strain ε, respectively. Fig. 6c shows that NC hydrogel samples do not break even at a strain of close to 100% compression, and therefore, the nominal stress σ_{nom} increases continuously with increasing strain. However, the corresponding σ_{true}–ε plots of the hydrogels shown in Fig. 6d pass through maxima indicating the onset of a microscopic failure in the gel specimen. The nominal fracture stress σ_f and the

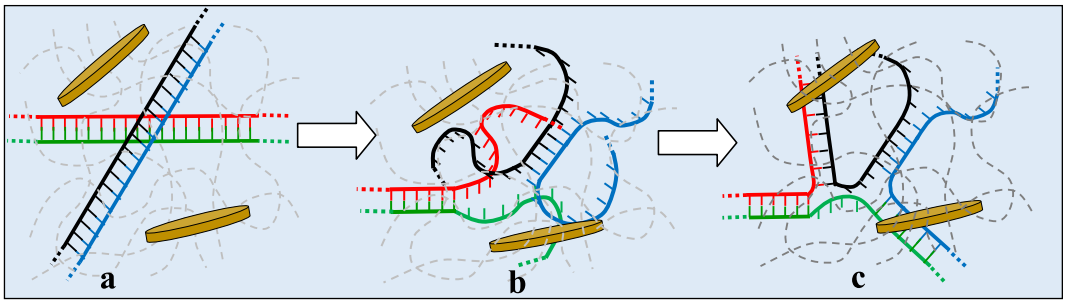

Fig. 5. Cartoon showing the conformational change of ds-DNA in NC hydrogels during heating (a→b) and cooling periods (b→c). Dashed gray lines and yellow disks represent PNIPA chains and Laponite particles while the ladder-like colored shapes represent ds-DNA strands. (For interpretation of the references to colour in this figure legend, the reader is referred to the web version of this article.)

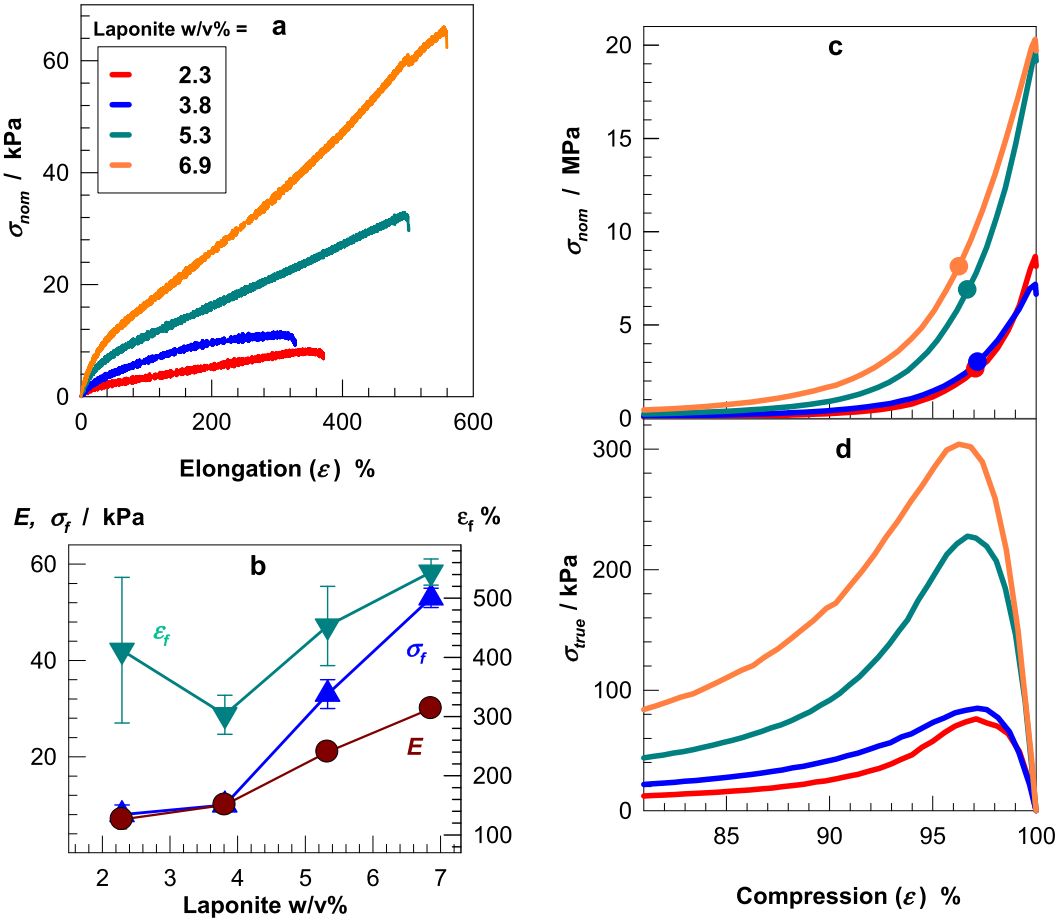

Fig. 6. (a) Nominal stress σ_{nom} – strain curves of NC hydrogels from elongation tests. (b): Young's modulus E, tensile fracture stress σ_f, and fracture strain ε_f of NC hydrogels plotted against the Laponite content. (c) Nominal σ_{nom} and trues stresses σ_{nom} plotted against the compression of NC hydrogels. Laponite contents are indicated.

compression ε_f at failure calculated from the maxima in σ_{true}–λ plots are indicated in Fig. 4c by the circles. NC hydrogels sustain up to 96% compressions and 2.4–8.1 MPa compressive stresses. Thus, as compared to the chemical cross-linking of DNA, the nanocomposite approach is very effective to produce mechanically strong ds-DNA hydrogels.

3.4. Swelling behavior of the hydrogels

To determine the swelling kinetics of NC hydrogels in water and their temperature sensitivity in the equilibrium swollen state, the gel specimens were immersed in water at 23 °C for at least 15 days whereby the water was replaced several times. The gel fraction W_g was found to be close to unity revealing that the monomer NIPA, DNA, and Laponite in the feed are converted almost completely into a water-insoluble hybrid polymer. Fig. 7a shows the swelling kinetic profiles of the hydrogels where the relative weight m_{rel} and volume swelling ratios V_{rel} are plotted against the swelling time. Both m_{rel} and V_{rel} first rapidly increase with the swelling time and, after passing maxima, they again decrease to attain the equilibrium

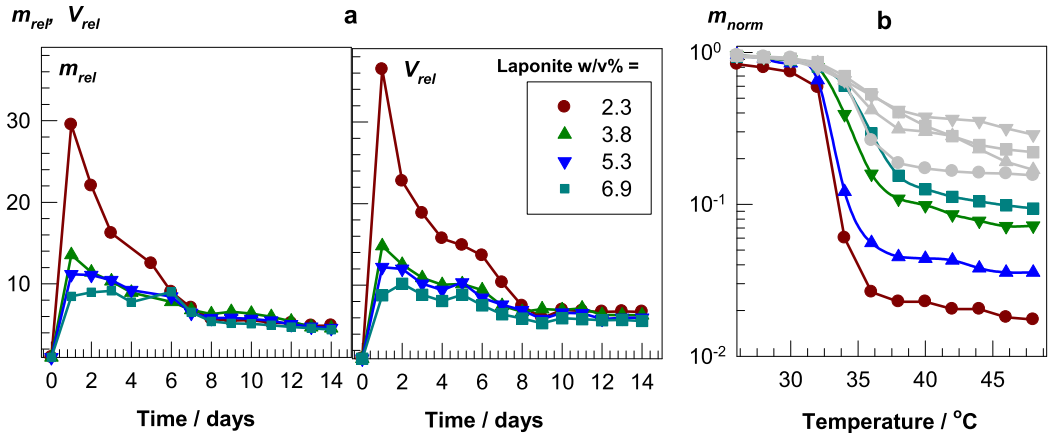

Fig. 7. (**a**): Relative weight m_{rel} and volume swelling ratio V_{rel} of the hydrogels plotted against the swelling time in water. Laponite contents are indicated. (**b**): The normalized swelling ratio m_{norm} of the hydrogels equilibrium swollen in water plotted against the temperature. The mass of the gel is normalized with respect to its mass at 20 °C. Laponite = 2.3 (●), 3.8 (▲), 5.3 (▼), and 6.9 w/v% (■). Gray symbols represent the data of NC hydrogels prepared in the absence of DNA.

values (Fig. S1). Such an unusual swelling kinetics has recently been reported for NC hydrogels prepared in the absence of DNA [59,60]. This behavior was first observed by Can et al. at Laponite concentrations above its critical overlap concentration (4.5 ± 1 w/v%) [59]. The authors attributed this behavior to the disintegration of clay agglomerates during the gel swelling so that new free sites on particle surfaces are generated. These free sites are then covered by polymer chains leading to an increase in the cross-link density and hence a decrease in the gel volume during swelling. Ren et al. explained this phenomenon with the release of sodium ions from the gel network during swelling [60]. However, as compared to these previous works, the extent of mass or volume increase during the initial swelling period is much larger for the present hydrogels containing DNA. Moreover, at Laponite contents below 4 w/v%, nanocomposite hydrogels without DNA exhibit usual swelling kinetics where the gel swells up to a critical time and then attains a constant mass. In contrast, present hydrogels exhibit the largest maximum swelling at Laponite contents below 4 w/v% (Fig. 7a). Because the release of DNA from the hydrogel into the surrounding water can be responsible for the appearance of maxima in the swelling curves, as in the case of non-ionic hydrogels containing ionic surfactants [36], we determined DNA concentration in water surrounding the gel samples using fluorescence measurements. The results showed that at least 98% ds-DNA remain in the hydrogels during the swelling process. Thus, DNA release is not responsible for the initial swelling period of the hydrogels. We attribute the large increase in the mass and volume of the hydrogels during the initial swelling period to the highly entangled state of DNA strands and PNIPA chains in the hydrogels. The rearrangements of the polymer chains and Laponite particles during the course of swelling increases the number of contacts between the clay particles and polymer segments leading to increasing cross-link density and decreasing swelling ratio of the hydrogels at long times.

The relative swelling ratios m_{rel} and V_{rel} of NC hydrogels in equilibrium with water are 5 ± 1 and 6.2 ± 0.5, respectively, and they slightly decrease within this range as the Laponite content is increased due to the simultaneously increase in the cross-link density. These swelling ratios are larger than those of NC hydrogels prepared in the absence of DNA exhibiting $m_{rel} = 3.7 \pm 0.8$ and $V_{rel} = 4 \pm 1$ in equilibrium with water. Because the degree of swelling increases with increasing charge density of the hydrogels [61], the presence of DNA counterions in the present hydrogels seems to be responsible for their excess swelling over the swelling of NC hydrogels without DNA. The temperature sensitivity of the hydrogels in equilibrium with water is represented in Fig. 7b where the normalized swelling ratio m_{norm} of the hydrogels in water are plotted against the water temperature. For comparison, the data obtained from NC hydrogels prepared in the absence of DNA are also shown in the figure by the gray symbols. The results reveal that the hydrogels undergo a deswelling transition above 32 °C, as reported for conventional PNIPA hydrogels [54,55]. Moreover, the hydrogels with a low Laponite content (2.3 and 3.8 w/v%) deswell rapidly at the transition region with one to two orders of magnitude change in the gel mass. As compared to the present hydrogels, those prepared in the absence of DNA exhibit only a small change in the gel mass during the deswelling transition. The drastic deswelling of NC hydrogels containing DNA with increasing temperature above 32 °C is expected due to the counterions of DNA in the PNIPA/DNA network. Thus, at low temperatures the osmotic pressure due to the phosphate ions of DNA inside the hydrogel dominates over the hydrophobic attractive interactions between the isopropyl groups of the PNIPA chains. As a result, the hydrogels are in a swollen state at low temperatures. With rising temperature above 32 °C, the hydrophobic interactions begin to dominate the swelling equilibrium leading to the collapse of the NC hydrogel. The results indicate that both the kinetics of gel swelling and the volume phase transition behavior in response to temperature changes are affected by the presence of DNA in NC hydrogels.

4. Conclusions

We presented a non-covalent approach to prepare high-strength DNA hydrogels with temperature sensitivity. The hydrogels consist of a 3D network of interconnected linear PNIPA chains and ds-DNA strands together with Laponite nanoparticles acting as a multifunctional dynamic cross-links. They were prepared by free-radical polymerization of *N*-isopropylacrylamide (NIPA) in aqueous Laponite dispersions containing ds-DNA in a highly entangled state. It was found that the native double-stranded DNA conformation is preserved during the formation of nanocomposite hydrogels. The elastic modulus of the hydrogels subjected to heating/cooling cycles between below and above the melting temperature of ds-DNA drastically increases due to the thermally induced denaturation and renaturation of ds-DNA within the physical network. The hydrogels prepared at various Laponite contents display the characteristics of

both poly(n-isopropylacrylamide) and ds-DNA e.g., temperature sensitivity, denaturation and renaturation of double-stranded DNA strands, and they exhibit a high tensile fracture stress (up to 53 kPa) and elongation to break (up to 544%). Such hydrogels are a good candidate to make use of the characteristics of both DNA and PNIPA in a diverse range of biomedical and biological applications.

Acknowledgments

This work was supported by the Scientific and Technical Research Council of Turkey (TUBITAK), KBAG 114Z312, and by Istanbul Technical University Scientific Research Project (ITU-BAP). Project No: 39773. OO thanks the Turkish Academy of Sciences (TUBA) for the partial support.

Appendix A. Supplementary data

Supplementary data related to this article can be found at http://dx.doi.org/10.1016/j.polymer.2016.08.041.

References

[1] J. Xu, T.H. LaBean, S.L. Craig, DNA structures and their applications in nanotechnology, in: A. Ciferri (Ed.), Supramolecular Polymers, CRC Press, Boca Raton, FL, 2004, pp. 445–480.
[2] V.A. Bloomfield, D.M. Crothers, I. Tinoco Jr., Nucleic Acids: Structures, Properties, and Functions, University Science Books, Sausalito, 2000.
[3] O. Okay, DNA hydrogels: new functional soft materials, J. Polym. Sci. B Polym. Phys. 49 (2011) 551–556.
[4] F.E. Alemdaroglu, A.Hermann, DNA meets synthetic polymers – highly versatile hybrid materials, Org. Biomol. Chem. 5 (2007) 1311–1320.
[5] Y. Murakami, M. Maeda, DNA-responsive hydrogels that can shrink or swell, Biomacromolecules 6 (2005) 2927.
[6] N. Ishizuka, Y. Hashimoto, Y. Matsuo, K. Ijiro, Highly expansive DNA hydrogel films prepared with photocrosslinkable poly(vinyl alcohol), Colloids Surf. A 284–285 (2006) 440.
[7] N. Dave, M.Y. Chan, P-J.J. Huang, B.D. Smith, J. Liu, Regenerable DNA-functionalized hydrogels for ultrasensitive, instrument-free mercury(II) detection and removal in water, J. Am. Chem. Soc. 132 (2010) 12668–12673.
[8] A. Zinchenko, Y. Miwa, L.I. Lopatina, V.G. Sergeyev, S. Murata, DNA hydrogel as a template for synthesis of ultrasmall gold nanoparticles for catalytic applications, ACS Appl. Mater. Interfaces 6 (2014) 3226–3232.
[9] A.S. Hoffman, Hydrogels for biomedical applications, Adv. Drug Deliv. Rev. 54 (2002) 3–12.
[10] B.V. Slaughter, S.S. Khurshid, O.Z. Fisher, A. Khademhosseini, N.A. Peppas, Hydrogels in regenerative medicine, Adv. Mater 21 (2009) 3307–3329.
[11] H. Matsuno, J.-I. Nakahara, K. Tanaka, Dynamic mechanical properties of solid films of deoxyribonucleic acid, Biomacromolecules 12 (2011) 173–178.
[12] M.J. Waring, DNA modification and cancer, Annu. Rev. Biochem. 50 (1981) 159–192.
[13] J.B. Chaires, Dissecting the free energy of drug binding to DNA, Anti-Cancer Drug Des. 11 (1996) 569–580.
[14] J.B. Chaires, Drug-DNA interactions, Curr. Opin. Struct. Biol. 8 (1998) 314–320.
[15] L.S. Lerman, Structural considerations in the interaction of DNA and acridines, J. Mol. Biol. 3 (1961) 18–30.
[16] R. Palchaudhuri, P.J. Hergenrother, DNA as a target for anticancer compounds: methods to determine the mode of binding and the mechanism of action, Curr. Opin. Biotechn 18 (2007) 497–503.
[17] P. Karacan, O. Okay, Ethidium bromide binding to DNA cryogels, React. Funct. Polym. 73 (2013) 442–450.
[18] T. Amiya, T. Tanaka, Phase transitions in crosslinked gels of natural polymers, Macromolecules 20 (1987) 1162.
[19] F. Horkay, P.J. Basser, Osmotic observations on chemically cross-linked DNA gels in physiological salt solutions, Biomacromolecules 5 (2004) 232–237.
[20] D. Costa, P. Hansson, S. Schneider, M.G. Miguel, B. Lindman, Interaction between covalent DNA gels and a cationic surfactant, Biomacromolecules 7 (2006) 1090–1095.
[21] S.H. Um, J.B. Lee, N. Park, S.Y. Kwon, C.C. Umbach, D. Luo, Enzyme-catalysed assembly of DNA hydrogel, Nat. Mater. 5 (2006) 797–801.
[22] D. Costa, M.G. Miguel, B. Lindman, Effect of additives on swelling of covalent DNA gels, J. Phys. Chem. B 111 (2007) 8444–8452.
[23] D. Costa, M.G. Miguel, B. Lindman, Responsive polymer gels: double-stranded versus single-stranded DNA, J. Phys. Chem. B 111 (2007) 10886–10896.
[24] F. Topuz, O. Okay, Rheological behavior of responsive DNA hydrogels, Macromolecules 41 (2008) 8847–8854.
[25] F. Topuz, O. Okay, Formation of hydrogels by simultaneous denaturation and cross-linking of DNA, Biomacromolecules 10 (2009) 2652–2661.
[26] N. Orakdogen, B. Erman, O. Okay, Evidence of strain hardening in DNA gels, Macromolecules 43 (2010) 1530–1538.
[27] Y. Xing, E. Cheng, Y. Yang, P. Chen, T. Zhang, Y. Sun, Z. Yang, D. Liu, Self-assembled DNA hydrogels with designable thermal and enzymatic responsiveness, Adv. Mater 23 (2011) 1117–1121.
[28] J.S. Kahn, A. Trifonov, A. Cecconello, W. Guo, C. Fan, I. Willner, Integration of switchable DNA-based hydrogels with surfaces by the hybridization chain reaction, Nano Lett. 15 (2015) 7773–7778.
[29] C. Li, M.J. Rowland, Y. Shao, T. Cao, C. Chen, H. Jia, X. Zhou, Z. Yang, O.A. Scherman, D. Liu, Responsive double network hydrogels of interpenetrating DNA and CB[8] host–guest supramolecular Systems, Adv. Mater 27 (2015) 3298–3304.
[30] P. Karacan, H. Cakmak, O. Okay, Swelling behavior of physical and chemical DNA hydrogels, J. Appl. Polym. Sci. 128 (2013) 3330–3337.
[31] Y. Tanaka, K. Fukao, Y. Miyamoto, Fracture energy of gels, Eur. J. Phys. E 3 (2000) 395–401.
[32] H.R. Brown, A model of the fracture of double network gels, Macromolecules 40 (2007) 3815–3818.
[33] A.M.S. Costa, J.F. Mano, Extremely strong and tough hydrogels as prospective candidates for tissue repair – a review, Eur. Polym. J. 72 (2015) 344–364.
[34] J.P. Gong, Y. Katsuyama, T. Kurokawa, Y. Osada, Double-network hydrogels with extremely high mechanical strength, Adv. Mater 15 (2003) 1155–1158.
[35] J.P. Gong, Why are double network hydrogels so tough? Soft Matter 6 (2010) 2583–2590.
[36] D.C. Tuncaboylu, M. Sahin, A. Argun, W. Oppermann, O. Okay, Dynamics and large strain behavior of self-healing hydrogels with and without surfactants, Macromolecules 45 (2012) 1991–2000.
[37] U. Gulyuz, O. Okay, Self-healing poly(acrylic acid) hydrogels with shape memory behavior of high mechanical strength, Macromolecules 47 (2014) 6889–6899.
[38] K. Haraguchi, T. Takehisa, Nanocomposite hydrogels: a unique organic–inorganic network structure with extraordinary mechanical, optical, and swelling/de-swelling properties, Adv. Mater 14 (2002) 1120–1124.
[39] K. Haraguchi, R. Farnworth, A. Ohbayashi, T. Takehisa, Compositional effects on mechanical properties of nanocomposite hydrogels composed of poly(N,N-dimethylacrylamide) and clay, Macromolecules 36 (2003) 5732–5741.
[40] K. Haraguchi, T. Takehisa, S. Fan, Effects of clay content on the properties of nanocomposite hydrogels composed of poly(N-isopropylacrylamide) and clay, Macromolecules 35 (2002) 10162–10171.
[41] K. Haraguchi, H.-J. Li, Mechanical properties and structure of polymer–clay nanocomposite gels with high clay content, Macromolecules 39 (2006) 1898–1905.
[42] K. Haraguchi, H.-J. Li, K. Matsuda, T. Takehisa, E. Elliott, Mechanism of forming organic/inorganic network structures during in-situ free-radical polymerization in PNIPA–clay nanocomposite hydrogels, Macromolecules 38 (2005) 3482–3490.
[43] O. Okay, W. Oppermann, Polyacrylamide – clay nanocomposite hydrogels: rheological and light scattering characterization, Macromolecules 40 (2007) 3378–3387.
[44] N. Arfin, H.B. Bohidar, Ergodic-to-nonergodic phase inversion and reentrant ergodicity transition in DNA–nanoclay dispersions, Soft Matter 10 (2014) 149–156.
[45] A. Taki, B. John, S. Arakawa, M. Okamoto, Structure and rheology of nanocomposite hydrogels composed of DNA and clay, Eur. Polym. J. 49 (2013) 923–931.
[46] P.A. Wheeler, J. Wang, L.J. Mathias, Poly(methyl methacrylate)/Laponite nanocomposites: Exploring covalent and ionic clay modifications, Chem. Mater 18 (2006) 3937–3945.
[47] O.L.J. Virtanen, A. Mourran, P.T. Pinard, W. Richtering, Persulfate initiated ultra-low cross-linked poly(N-isopropylacrylamide) microgels possess an unusual inverted cross-linking structure, Soft Matter 12 (2016) 3919–3928.
[48] J. Gao, B.J. Frisken, Cross-linker-free N-isopropylacrylamide gel nanospheres, Langmuir 19 (2003) 5212–5216.
[49] Z. Grauer, D. Avnir, S. Yariv, Adsorption characteristics of rhodamine 6G on montmorillonite and laponite, elucidated from electronic absorption and emission spectra, Can. J. Chem. 62 (1984) 1889–1894.
[50] J.W. Davis, M.S. Kahl, T.D. Golden, Mechanistic study of cationic dye interactions with clay-polymer dispersions via metachromatic effect, aggregation, and surface charge, J. Appl. Polym. Sci. 40141 (2014).
[51] M. Grabolle, M. Starke, U. Resch-Genger, Highly fluorescent dye–nanoclay hybrid materials made from different dye classes, Langmuir 32 (2016) 3506–3513.
[52] S. Nandi, P. Routh, R.K. Layek, A.K. Nandi, Ethidium bromide-adsorbed graphene templates as a platform for preferential sensing of DNA, Biomacromolecules 13 (2012) 3181–3188.
[53] A. Mishra, M.K. Ekka, S. Maiti, Influence of ionic liquids on thermodynamics of small molecule–DNA interaction: the binding of ethidium bromide to Calf Thymus DNA, J. Phys. Chem. B 120 (2016) 2691–2700.
[54] Y. Hirokawa, T. Tanaka, Volume phase transition in a nonionic gel, J. Chem. Phys. 81 (1984) 6379–6380.
[55] S. Hirotsu, Coexistence of phases and the nature of first-order transition in poly(N-isopropylacrylamide) gels, Adv. Polym. Sci. 110 (1993) 1–26.
[56] M. Teodorescu, M. Andrei, G. Turturică, P.O. Stănescu, A. Zaharia, A. Sârbu, Novel thermoreversible injectable hydrogel formulations based on sodium alginate and poly(N-isopropylacrylamide), Int. J. Polym. Mater. Polym. Biomater. 64 (2015) 763–771.

[57] M. D'Este, M. Alini, D. Eglin, Single step synthesis and characterization of thermoresponsive hyaluronan hydrogels, Carbohydr. Polym. 90 (2012) 1378–1385.
[58] M. Kundu, S. Mallapragada, R.C. Larock, P.P. Kundu, Rheological properties of methylcellulose aqueous gels under dynamic compression: frequency sweep and validity of scaling law, J. Appl. Polym. Sci. 117 (2010) 2436–2443.
[59] V. Can, S. Abdurrahmanoglu, O. Okay, Unusual swelling behavior of polymer-clay nanocomposite hydrogels, Polymer 48 (2007) 5016–5023.
[60] H. Ren, M. Zhu, K. Haraguchi, Characteristic swelling–deswelling of polymer/clay nanocomposite gels, Macromolecules 44 (2011) 8516–8526.
[61] P.J. Flory, Principles of Polymer Chemistry, Cornell University Press, Ithaca, NY, 1953.